# *Improvement of LVRT and transient stability of power system with wind farms using coordination of FACTS and PSSs controllers*

Amir Movahedi
*Department of Electrical and Computer Engineering, University of Kashan*
Kashan, Iran
a.movahedi@grad.kashanu.ac.ir

Abolfazl Halvaei Niasar
*Department of Electrical and Computer Engineering, University of Kashan*
Kashan, Iran
halvaei@kashanu.ac.ir

G.B. Gharehpetian
*Electrical Engineering Department*
*Amirkabir University of Technology*
Tehran, Iran
grptian@aut.ac.ir

***Abstract*—This paper presents the comparison of static synchronous series compensator (SSSC) and static synchronous compensator (STATCOM) performance on transient stability and low voltage ride through (LVRT) improvement of a multi-machine power system connected with wind farms. Also, power system stabilizers (PSSs) are installed on four synchronous machines. It is generally accepted that there is a threat to the stability of power systems with the penetration of wind farm. Therefore, in order to improve LVRT and transient stability in power system, the paper proposes using of PI controllers in wind farms and combination of the PSS and FACTS controllers. Also, In the present paper gravitational search algorithm (GSA) has been applied for controllers design.**

***Keywords*—GSA, LVRT, SSSC, STATCOM, Wind farm.***

## I. INTRODUCTION

The share of wind power with respect to total installed power capacity is increasing worldwide. Currently, DFIG is the most frequently used generator for wind turbines (WTs) due to its advantages [1-3]. The stator of the DFIG is directly connected to the grid while its rotor is connected through an AC/DC/AC converter. When the grid voltage dip occurs, the stator flux cannot be changed and, therefore, stator windings will induce a DC component of the stator flux which also contains a negative-sequence component during asymmetrical grid voltage dips.

Since the capacity of the DFIG converter is only 25% to 30% [2], the grid fault can easily cause rotor overvoltage or over-current, which makes the converter a direct threat to the safety of the WT operation. Consequently, an effective control should be exerted in order to prevent stator and rotor inrush currents as well as overvoltage and torque oscillations, and to allow the DFIG-based WT to remain connected to the grid during faults. The proposed solution involves the use of PI controllers in rotor-side and grid-side controllers and application of FACTS devices on the transmission line.

Flexible AC transmission system (FACTS) devices can be used to control power flow and enhance system stability [4, 5]. This paper investigates the improvement of the transient stability of a two-area power system with wind farms, using an SSSC and STATCOM.

SSSC is utilized for power flow control, voltage stability, and phase-angle stability. The benefit of SSSC over conventional controllable series capacitors is that SSSC induces both capacitive and inductive series compensating voltages on a line [6, 7]. STATCOM can be defined as a synchronous static generator which operates as a shuntly-connected reactive power static compensator. Its output current can be fully controlled in both the capacitive and inductive range, independently of AC network voltage [8, 9].

Numerous studies have been conducted in the field of simultaneous coordinated design of PSS and FACTS controllers [10, 11]. Several modern heuristic tools that facilitate the solution of optimization problems which were previously difficult or impossible to address have evolved in the last two decades. These tools include, among others, evolutionary computation, simulated annealing, tabu search, and particle swarm. The gravitational search algorithm (GSA), emerged as promising algorithms for handling optimization problems. This algorithm is gaining popularity within the research community as design tool and problem-solver because of their versatility and capability for optimization in complex multimodal search spaces applied to non-differentiable cost functions [12, 13].

## II. FACTS DEVISES

### A. SSSC

SSSC is a kind of variable impedance type series compensator [6, 7]. A SSSC consists of a DC/AC switched mode converter which is a voltage source inverter (VSI) converting voltage from DC to AC and generating compensating voltage, a DC capacitor for supplying DC link voltage to the VSI, and an injection transformer for stepping up the output voltage of the VSI to the line. The transformer is connected in series with the transmission line. It also provides electrical isolation environment to the VSI. The VSI is operated with fast switching devices at high switching frequency for fast response [6, 7].

The typical SSSC-damping controller structure is illustrated in Fig. 1. In this paper, K and time constants $T_1$, $T_2$, $T_3$, and $T_4$ can be calculated using GSA.

978-1-7281-1508-5/19/$31.00 ©2019 IEEE

### B. STATCOM

STATCOM in a steady-state operating regime which replicates the operating characteristics of a rotating synchronous compensator. The basic electronic block of a STATCOM is a voltage-sourced converter that converts a DC voltage at its input terminals into a three-phase set of AC voltages at a fundamental frequency with a controllable magnitude and phase angle [8, 9]. A STATCOM can be used for voltage regulation in a power system, having as an ultimate goal an increase in transmittable power as well as improvements of steady-state transmission characteristics and the overall stability of the system. The commonly used lead–lag structure depicted in Fig. 1 is chosen in this study as a STATCOM-based damping controller. K and time constants $T_1$, $T_2$, $T_3$, and $T_4$ can be calculated using GSA.

## III. PSS AND SYSTEM MODEL

In order to power system stability enhancement by FACTS, the installation of PSS is effective. A PSS installed in the excitation system of the synchronous generator to improves the small-signal power system stability by damping out low frequency oscillations in the power system. It does that by providing supplementary perturbation signals in a feedback path to the alternator excitation system [14, 15]. The typical PSS controller is illustrated in Fig. 1.

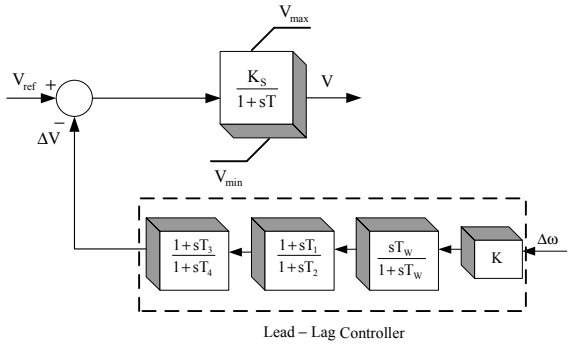


Figure 1. Lead-lag controller

Fig. 2 illustrates the structure of the proposed system [11]. In Fig. 2, the power system consists of different areas: Two synchronous generators $G_1$ and $G_2$, and a wind farm based on $DFIG_1$ are in the first area, while $G_3$, $G_4$, and $DFIG_2$ are in the second area. $G_1$ and $G_3$ are 900 MVA; $G_2$ and $G_4$ are 650 MVA; $DFIG_1$ and $DFIG_2$ are 200 MW. SSSC in the second line are between bus 9 and bus 12, and STATCOM is connected in bus 9. Moreover, PSS is installed on four synchronous generators ($G_1$, $G_2$, $G_3$, and $G_4$).

### A. Wind Farms

The wind farm basically consists of DFIG, a wind turbine with a drive train system, RSC, GSC, DC-link capacitor, pitch controller, coupling transformer, and protection system as shown in [1, 2]. The wind turbine with the DFIG system is an induction-type generator in which the stator windings are directly connected to the three-phase grid, and the rotor windings are fed through three-phase back-to back insulated-gate bipolar transistor (IGBT)-based pulse width modulation (PWM) converters. The dynamics of the DFIG is represented by a fourth-order state-space model using the synchronously rotating reference frame (qd-frame) as given in (1)-(4) [1-3].

$$V_{qs} = r_s I_{qs} + \omega_e \lambda_{ds} + d\lambda_{qs}/dt \quad (1)$$

$$V_{ds} = r_s I_{ds} - \omega_e \lambda_{qs} + d\lambda_{ds}/dt \quad (2)$$

$$V_{qr} = r_r I_{qr} + (\omega_e - \omega_r)\lambda_{dr} + d\lambda_{qr}/dt \quad (3)$$

$$V_{dr} = r_r I_{dr} + (\omega_e - \omega_r)\lambda_{qr} + d\lambda_{dr}/dt \quad (4)$$

where, $V_{qs}$, $V_{ds}$, $V_{qr}$, and $V_{dr}$ are the q- and d-axis stator and rotor voltages, respectively; $I_{qs}$, $I_{ds}$, $I_{qr}$, and $I_{dr}$ are the q- and d-axis stator and rotor currents, respectively; $\lambda_{qs}$, $\lambda_{ds}$, $\lambda_{qr}$ and $\lambda_{dr}$ are the q- and d-axis stator and rotor fluxes, respectively; $\omega_e$ is the angular velocity of the synchronously rotating reference frame; and $\omega_r$ is rotor angular velocity, respectively. The flux linkage equations are given as [1, 3].

$$\lambda_{qs} = L_s I_{qs} + L_m I_{qr} \quad , \quad \lambda_{ds} = L_s I_{ds} + L_m I_{dr} \quad (5)$$

$$\lambda_{qr} = L_m I_{qs} + L_r I_{qr} \quad , \quad \lambda_{dr} = L_m I_{ds} + L_r I_{dr} \quad (6)$$

where $L_s$, $L_r$, and $L_m$ represents the stator, rotor, and mutual inductances, respectively. Assuming negligible power losses in stator and rotor resistances, the active and reactive power outputs from stator and rotor sides are given as:

$$P_s = -(3/2)(V_{qs} I_{qs} + V_{ds} I_{ds}) \quad , \quad Q_s = -(3/2)(V_{qs} I_{ds} - V_{ds} I_{qs}) \quad (7)$$

$$P_r = -(3/2)(V_{qr} I_{qr} + V_{dr} I_{dr}) \quad , \quad Q_r = -(3/2)(V_{qr} I_{dr} - V_{dr} I_{qr}) \quad (8)$$

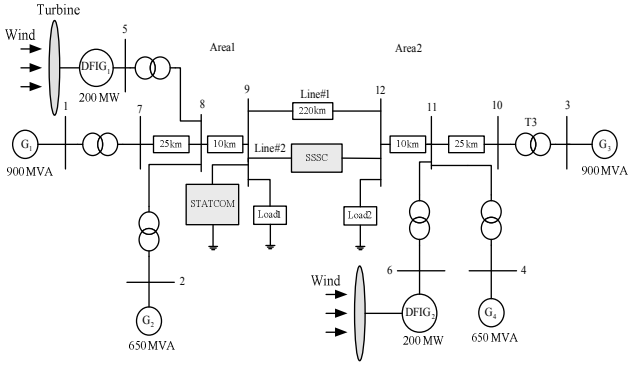


Figure 2. Power system with wind farms

The total active and reactive power generated by DFIG is:

$$P_{Total} = P_s + P_r \quad , \quad Q_{Total} = Q_s + Q_r \quad (9)$$

If $P_{Total}$ and/or $Q_{Total}$ is positive, DFIG is supplying power to the power grid; otherwise, it is drawing power from the grid. $T_e$ is the electromagnetic torque generated by the machine, which can be written in terms of flux linkages and currents as follows:

$$T_e = (3/2)(\lambda_{qs} I_{ds} - \lambda_{ds} I_{qs}) \quad (10)$$

### B. Control Systems of Wind Farms

The rotor-side converter (RSC) is applied to control the wind turbine output power and the voltage or reactive power measured at grid terminals. Power is controlled in order to

follow a pre-defined power speed characteristic (tracking characteristic) [1, 3]. The control system is presented in Fig. 3a.

The grid-side converter (GSC) is utilized to regulate the DC bus capacitor voltage. The control system is depicted in Fig. 3b [1, 3]. The GSC control feeds the DC voltage regulator from the difference between $V_{dc}$ and $V_{dc}$ reference, and transfers it into the d-q axis current or the current regulator by the PI controller. Then, using the PI controller, it transfers the regulator again into the d-q axis voltage with the electrical equation of Park's transformation [1].

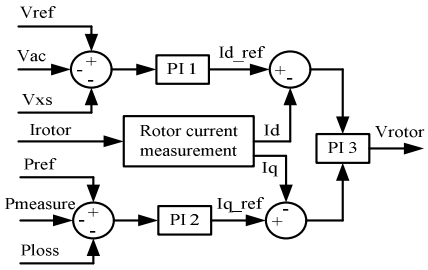


(a). Schematic diagram of RSC

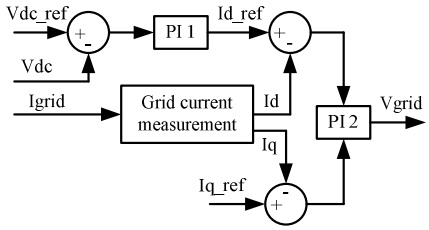


(b). Schematic diagram of GSC

Figure 3. Wind farm controllers structure

According to the new grid codes, WTs must remain connected to the grid and supply reactive power to guarantee the grid voltage during grid faults. This ability of WTs is called the fault ride through (FRT) capability and, for voltage dips, the LVRT capability [16]. LVRT depends on the magnitude of voltage drop at the point of common coupling (PCC) during fault and the time taken by the grid system to recover to the normal state [16]. A summary of the voltage profile for ride-through capabilities in the grid codes is presented in Fig. 5 [16]. Only when the grid voltage goes below the curves are the turbines allowed to be disconnected. Moreover, when the voltage is in the special area, the turbines should supply reactive power.

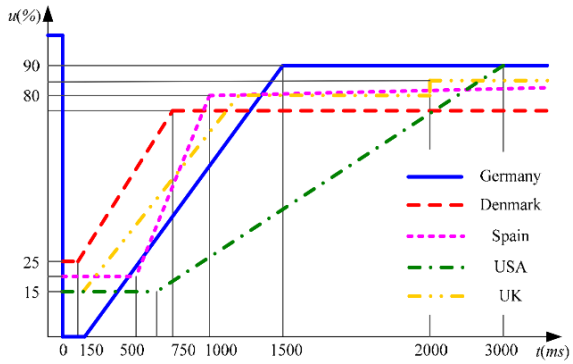


Figure 4. Voltage profile for LVRT in different countries

## IV. GRAVITATIONAL SEARCH ALGORITHM (GSA)

The objective function can be defined as:

$$J = \sum \int_0^{t1} t\left|\Delta\omega(t, X)\right|dt \tag{11}$$

The GSA is based on Newton's theory. The position of the mass corresponds to a solution to the problem, and its gravitational and inertial masses are determined using a fitness function. In other words, each mass presents a solution, and the algorithm is navigated by properly adjusting the gravitational and inertial masses. For a system with N-agent (masses), the $i^{th}$ position of an agent $X_i$ is defined by [12, 13]:

$$X_i = (X_i^1, ..., X_i^d, ..., X_i^N) \quad \text{For } i = 1,2,..., N \tag{12}$$

At a specific time 't', the force acting on mass 'i' from mass 'j' is defined as follows [12, 13]:

$$F_{ij}^d(t) = G(t)\frac{M_{pi}(t)\times M_{aj}(t)}{R_{ij}(t)+\varepsilon}[X_j^d(t) - X_i^d(t)] \tag{13}$$

where $M_{aj}$ represents the active gravitational mass related to agent 'j'. To give a stochastic characteristic to the GSA algorithm, it is assumed that the total force acting on agent 'i' in dimension 'd' is a random weight sum of the 'd'th components of the forces exerted from other agents as [12, 13]:

$$F_i^d(t) = \sum_{j=1, j\neq i}^{N} rand_j F_{ij}^d(t) \quad , \quad a_i^d(t) = \frac{F_i^d(t)}{M_{ii}(t)} \tag{14}$$

where $M_{ii}$ (t) is the inertia mass of the 'i'th agent. Therefore, its position and velocity can be calculated as follows [12, 13]:

$$v_i^d(t+1) = rand_i \times v_i^d(t) + a_i^d(t) \tag{15}$$

$$x_i^d(t+1) = x_i^d(t) + v_i^d(t+1) \tag{16}$$

The gravitational and inertial masses are updated by the following equations [12, 13]:

$$M_{ai} = M_{pi} = M_{ii} = M_i \quad , \quad M_i(t) = m_i(t) / \sum_{j=1}^{N} m_j(t) \tag{17}$$

$$m_i(t) = \frac{fit_i(t) - worst(t)}{best(t) - worst(t)} \tag{18}$$

where $fit_i(t)$ represents the fitness value of the agent 'i' at time 't', and best(t) and worst(t) are defined as follows:

$$best(t) = \min fit_j(t) \quad , \quad worst(t) = \max fit_j(t) \tag{19}$$

## V. SIMULATION RESULTS

The values for the optimized parameters are shown in Tables I and II.

TABLE I. THE VALUES OF FACTS CONTROLLERS WITH GSA

| | K [pu] | $T_1$ [s] | $T_2$ [s] | $T_3$ [s] | $T_4$ [s] |
|---|---|---|---|---|---|
| **SSSC** | 16.6391 | 0.3989 | 0.3905 | 0.4015 | 0.3764 |
| **Statcom** | 22.9684 | 0.5976 | 0.2907 | 0.5069 | 0.3967 |

TABLE II. THE VALUES OF PSS CONTROLLERS WITH GSA

| Parameters | Value | Parameters | Value | Range |
|---|---|---|---|---|
| $K_{G1}$ [pu] | 19.9803 | $K_{G3}$ [pu] | 26.6371 | 20-60 |
| $K_{G2}$ [pu] | 22.3041 | $K_{G4}$ [pu] | 26.0196 | 20-60 |
| $T_{1G1}$=$T_{3G1}$ [s] | 0.6531 | $T_{2G1}$=$T_{4G1}$ [s] | 0.4418 | 0.01-1 |
| $T_{1G2}$=$T_{3G2}$ [s] | 0.5891 | $T_{2G2}$=$T_{4G2}$ [s] | 0.4739 | 0.01-1 |
| $T_{1G3}$=$T_{3G3}$ [s] | 0.4691 | $T_{2G3}$=$T_{4G3}$ [s] | 0.4559 | 0.01-1 |
| $T_{1G4}$=$T_{3G4}$ [s] | 0.519 | $T_{2G4}$=$T_{4G4}$ [s] | 0.6391 | 0.01-1 |

In Fig. 5, the objective function with GSA converges to 0.0026 for gbest.

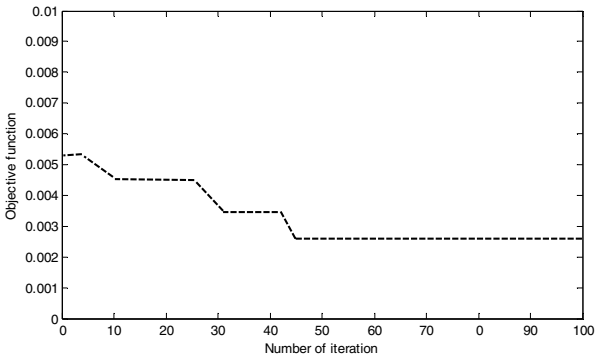


Figure 5. Convergence of the objective function for gbest

A three-phase line-to-ground fault in line 1 between bus 9 and bus 12 is simulated for 100 ms (Fig. 2). This fault has occurred in 1.2 s and is disappeared in 1.3 s. Speed, rotor angle, and output power of synchronous generators are presented in Figs. 6a-e, respectively. Considering Fig. 6, the system are unstable because a three-phase line-to-ground fault has occurred but are damped at about 5.5 s using STATCOM and PSS simultaneous controllers. The duration of damping in about 4 s and oscillations step down by the use of SSSC and PSS simultaneous controllers. It demonstrates the superiority and higher speed of SSSC than STATCOM.

The responses of the terminal voltage (PCC), active and reactive power of DFIG1 and 2, are presented in Figs. 7a-d, respectively. The voltage diped during the fault, where voltage can be significantly retained to around 1 pu using PI and FACTS controllers after clearing the fault. Considering Figs. 4 and 7a, without controllers, voltage collapse has occurred in the weak-grid condition and the LVRT grid code cannot be satisfied as the wind turbines have to be disconnected from the grid.

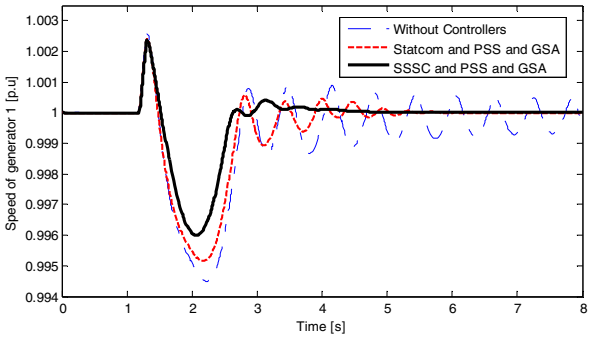


(a). Speed of generator 1

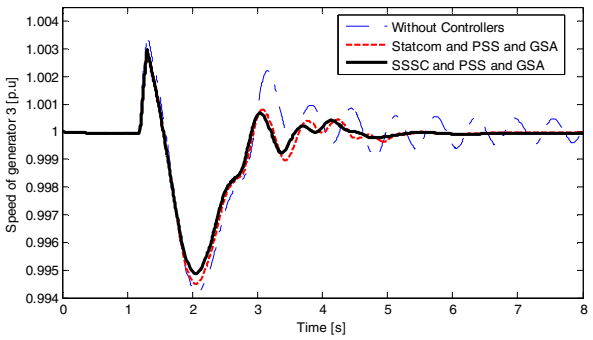


(b). Speed of generator 3

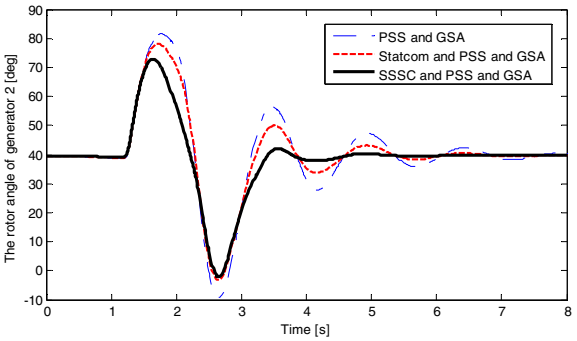


(c). The rotor angle of generator 2

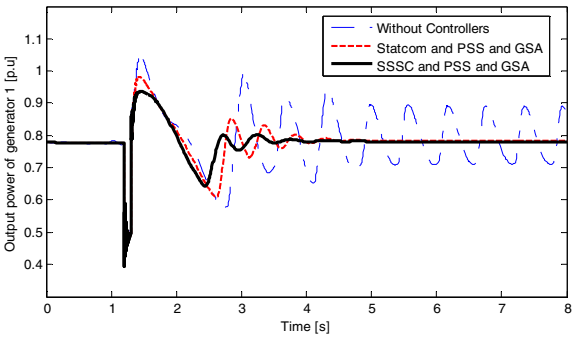


(d). Output power of generator 1

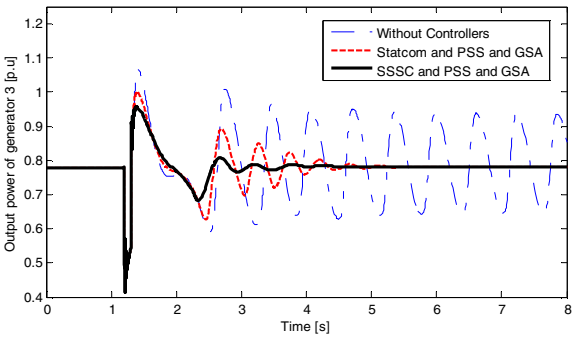


(e). Output power of generator 3

Figure 6. Simulation results of power system

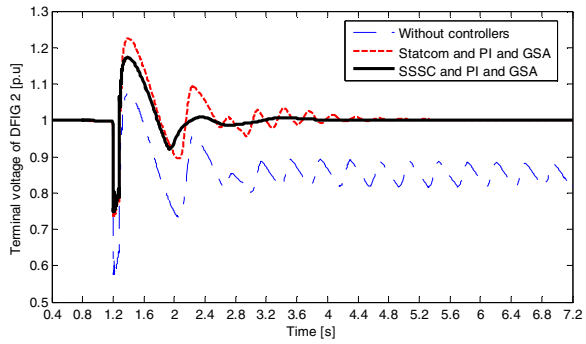


(a). Terminal voltage of DFIG 2

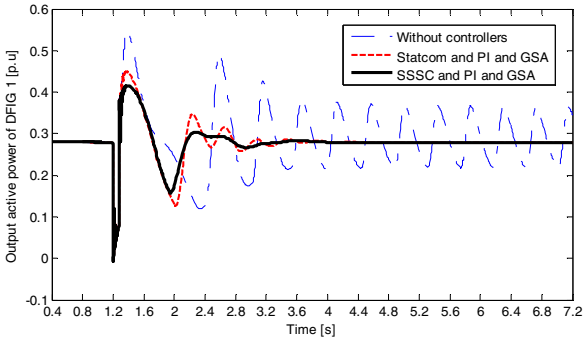


(b). Output active power of DFIG 1

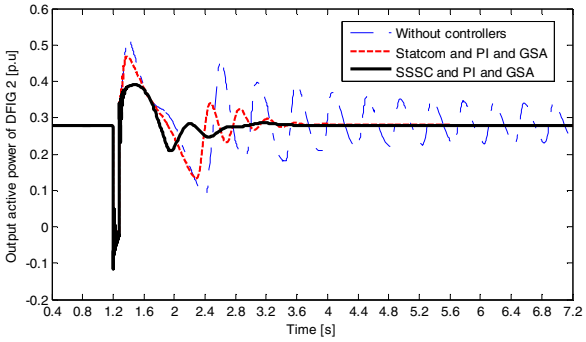


(c). Output active power of DFIG 2

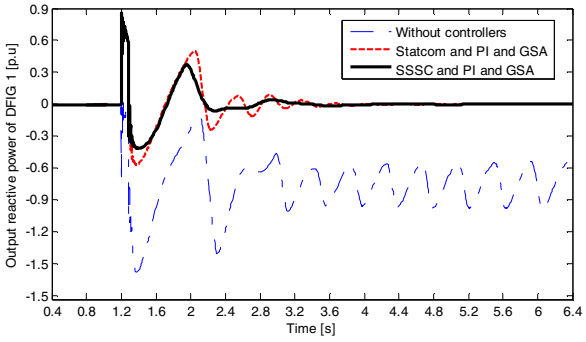


(d). Output reactive power of DFIG 1

Figure 7. Simulation results of wind farms

## VI. CONCULATION

In this paper, the power system stability enhancement via PI controllers and PSS and FACTS-based stabilizers when applied through coordinated application was discussed and investigated for a multi-machine power system in the presence of wind farms. Parameters of the proposed FACTS, PSS, and PI controllers were optimized using GSA. The system has become unstable following the three-phase line-to-ground fault; however, by the simultaneous application of STATCOM and PSS controllers, the stability of the system improves and its oscillations are damped. Using SSSC and PSS simultaneous controllers, oscillation and time damping have been decreased compared to STATCOM. Furthermore, the comparison of the simulated methods indicated that SSSC and PI controllers are the most reliable and effective LVRT capability enhancement methods for wind farms.

## REFERENCES

[1] H. Geng, G. Yang, “Small-signal stability of power system integrated with ancillary-controlled large-scale DFIG-based wind farm”, IET Renewable Power Generation, Vol. 11, pp. 1191-1198, July 2017.

[2] Y. Tang, Haibo He, “Power System Stability Control for a Wind Farm Based on Adaptive Dynamic Programming”, IEEE TRANSACTIONS ON SMART GRID, Vol. 6, pp. 166-177, Jan. 2015.

[3] B. Pokharel, “Modeling, control and analysis of a doubly fed induction generator based wind turbine system with voltage regulation”, Master of science electrical engineering technological university, Dec. 2011.

[4] E. Ghahremani, I. Kamwa, “Analysing the effects of different types of FACTS devices on the steady-state performance of the Hydro-Québec network”, IET Generation, Transmission & Distribution, Vol. 8, pp. 233-249, Feb. 2014.

[5] H. Nguyen-Duc, L. Dessaint, A.F. Okou, I. Kamwa, “A power oscillation damping control scheme based on bang-bang modulation of FACTS signals”, IEEE Trans. on Pow. Sys., Vol.25, No.4, pp.1918-1927, 2010.

[6] B. Ankitkumar, “A SSSC based damping controller for stability enhancement of power system”, IEEE/AEEICB, pp. 183-187, Feb. 2017.

[7] M. Eremia, Chen-Ching Liu, “Static Synchronous Series Compensator (SSSC)”, Wiley-IEEE Press eBook Chapters, 2016.

[8] L. Wang, C. Chang, “Stability Improvement of a Two-Area Power System Connected With an Integrated Onshoreo and Offshore Wind Farm Using a STATCOM”, IEEE Industry Applications Society, Vol. 53, pp. 867-877, Nov. 2016.

[9] Zhixing He, Fujun Ma, Qianming Xu, “Reactive Power Strategy of Cascaded Delta-Connected STATCOM Under Asymmetrical Voltage Conditions”, IEEE Journal of Emerging and Selected Topics in Power Electronics, Vol. 5, pp. 784-795, June 2017.

[10] X. Y. Bian, Yan Geng, Kwok L. Lo, “Coordination of PSSs and SVC Damping Controller to Improve Probabilistic Small-Signal Stability of Power System With Wind Farm Integration”, IEEE Transactions on Power Systems, Vol. 31, pp. 2371-2382, May 2016.

[11] M. B. Saleh, M. A. Abido, “Power system damping enhancement via coordinated design of PSS and TCSC in multi-machine power system”, IEEE/GCC, pp. 1-6, Mar. 2006.

[12] S. M. Abd Elazim, “Optimal SSSC design for damping power systems oscillations via Gravitational Search Algorithm”, International Journal of Electrical Power & Energy Systems, Vol. 82, pp. 161-168, Nov. 2016.

[13] B. Bhattacharyya, S. Kumar, “Approach for the solution of transmission congestion with multi-type FACTS devices”, IET Generation, Transmission & Distribution, Vol. 10, pp. 2802–2809, Aug. 2016.

[14] E. Dysko, W. E. Leithead, “Enhanced Power System Stability by Coordinated PSS Design”, IEEE Transactions on Power Systems, Vol. 25, pp. 413-442, Feb. 2010.

[15] X. Y. Bian, Yan Geng, Kwok L. Lo, “Coordination of PSSs and SVC Damping Controller to Improve Probabilistic Small-Signal Stability of Power System With Wind Farm Integration”, IEEE Transactions on Power Systems, Vol. 31, pp. 2371-2382, May 2016.

[16] M. Tsili, “A review of grid code technical requirements for wind farms”, school of Electrical and Computer Engineering, pp. 308-312, 2009.